Available online at www.sciencedirect.com

ScienceDirect

Biochimica et Biophysica Acta 1778 (2008) 1871–1880

Biochimica et Biophysica Acta BBA

www.elsevier.com/locate/bbamem

Review

OmpA: Gating and dynamics via molecular dynamics simulations

Syma Khalid, Peter J. Bond, Timothy Carpenter, Mark S.P. Sansom *

Department of Biochemistry, University of Oxford, South Parks Road, Oxford, OX1 3QU, UK

Received 6 April 2007; received in revised form 23 May 2007; accepted 25 May 2007
Available online 2 June 2007

Abstract

Outer membrane proteins (OMPs) of Gram-negative bacteria have a variety of functions including passive transport, active transport, catalysis, pathogenesis and signal transduction. Whilst the structures of ~25 OMPs are currently known, there is relatively little known about their dynamics in different environments. The outer membrane protein, OmpA from *Escherichia coli* has been studied extensively in different environments both experimentally and computationally, and thus provides an ideal test case for the study of the dynamics and environmental interactions of outer membrane proteins. We review molecular dynamics simulations of OmpA and its homologues in a variety of different environments and discuss possible mechanisms of pore gating. The transmembrane domain of *E. coli* OmpA shows subtle differences in dynamics and interactions between a detergent micelle and a lipid bilayer environment. Simulations of the crystallographic unit cell reveal a micelle-like network of detergent molecules interacting with the protein monomers. Simulation and modelling studies emphasise the role of an electrostatic-switch mechanism in the pore-gating mechanism. Simulation studies have been extended to comparative models of OmpA homologues from *Pseudomonas aeruginosa* (OprF) and *Pasteurella multocida* (PmOmpA), the latter model including the periplasmic C-terminal domain.

Keywords: Outer membrane protein; OmpA; Molecular dynamics; Homology model

Contents

1. Introduction

The outer membrane of Gram-negative bacteria serves as a protective barrier against the external environment whilst also controlling the influx and efflux of solutes. Outer membrane proteins (OMPs) found in bacterial outer membranes provide a variety of functions including passive and active transport, host–pathogen recognition, signal transduction, and catalysis. It has been predicted that 2–3% of the genes in Gram-negative bacteria encode integral OMPs [1]. However, to date only about 25 unique OMP structures have been solved by NMR or X-ray crystallography (http://blanco.biomol.uci.edu/Membrane_Proteins_xtal.html). In contrast to the α-helical fold of inner membrane proteins, OMPs have an overall β-barrel architecture. These barrels are composed of anti-parallel β-strands connected by short turns on the periplasmic side of the membrane, and by extended loops on the extracellular side [2]. The outer surface of

* Corresponding author. Tel.: +44 1865 275371; fax: +44 1865 275273.
E-mail address: mark.sansom@bioch.ox.ac.uk (M.S.P. Sansom).

0005-2736/$ - see front matter © 2007 Elsevier B.V. All rights reserved.
doi:10.1016/j.bbamem.2007.05.024

the barrels is invariably hydrophobic whilst the membrane–solvent interface is composed of predominantly amphipathic aromatic (i.e. tryptophan and tyrosine) residues. OMPs are found in the outer membranes (OM) of Gram-negative bacteria as well as in the cell envelopes of some Gram-positive bacteria. The OM is asymmetric in nature; the inner leaflet which faces the periplasmic space is composed of phospholipids and thus is similar in structure to the inner membrane [3]. In contrast, the outer leaflet is rather more complicated. It is composed of large lipopolysaccharide molecules (LPS). These are charged polysaccharides cross linked by divalent cations with multiple saturated fatty acid tails. The structure of LPS varies substantially from species to species and can even be modified within a single cell in response to changes in the local environment [4,5]. The low permeability of the OM results from the combination of highly charged sugars and tightly ordered hydrocarbon chains, and enables it to perform its major role of protecting the cell against toxic agents. However, to enable exchange of solute molecules between the periplasm and the environment, the OM is rendered selectively permeable to molecules smaller than ca. 1 kDa by the presence of pore-forming OMPs known as porins. The general porins provide a simple diffusion pathway across the membrane and have little substrate selectivity. They allow most solutes to enter while excluding dangerous toxins or proteases. A sub-class of substrate-specific channels also exists, for example maltoporin which exhibits selectivity for linear oligosaccharides.

Outer Membrane Protein A, (OmpA) from *Escherichia coli* is one of the most widely studied OMPs, both experimentally and computationally. It is one of the few membrane proteins whose structure has been solved both by X-ray crystallography (Fig. 1A) and by solution NMR in detergent micelles (Fig. 1B). The two other proteins for which similar structural data are available are PagP [6–8] and OmpX [9,10]; both are from *E .coli*.

OmpA is a small monomeric protein composed of two domains, connected by an 18 residue, proline-rich hinge region. Lying in the outer membrane is the N-terminal domain, an eight-stranded, ~170 residue, anti-parallel β-barrel. The crystal structures show that the β-strands are tilted on average by 45° relative to the barrel axis. The barrel has a cross-sectional diameter of 26 Å and a cylindrical length of 57 Å. The strands are connected by short turns on the periplasmic side and by more extended loops on the extracellular side. The C-terminal

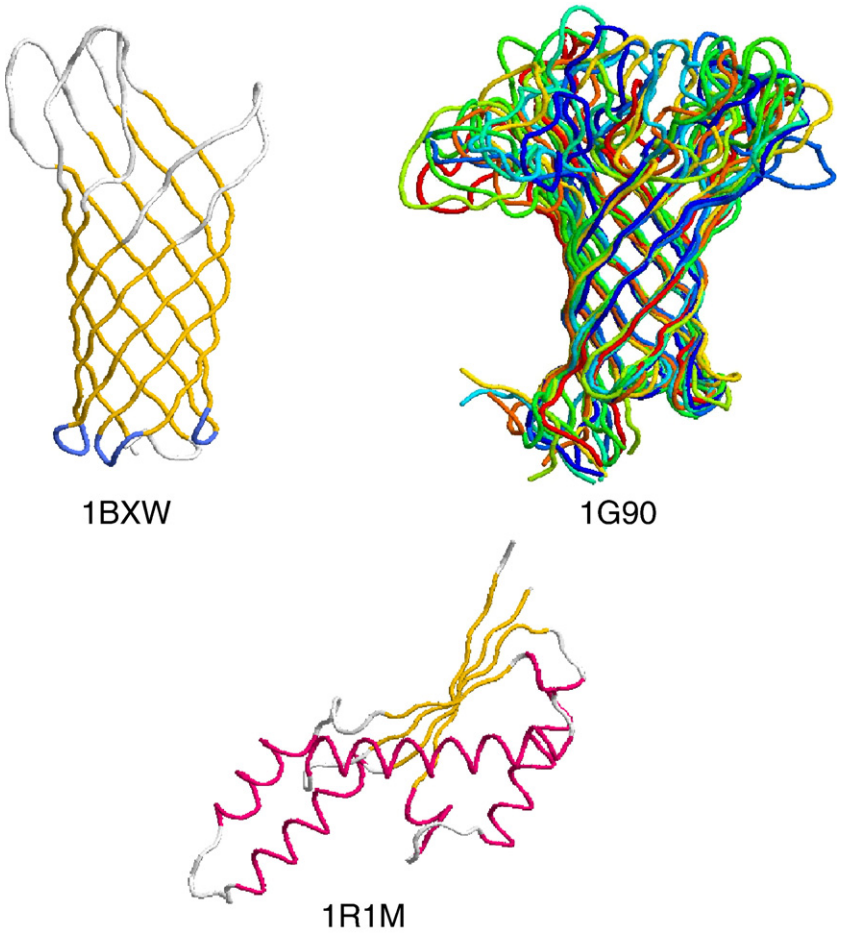

Fig. 1. X-ray and NMR structures of OmpA and related proteins. **1BXW** X-ray structure of the *E. coli* OmpA transmembrane (N-terminal) domain structure [36]. **1G90** Solution NMR structure of OmpA in dodecyl-phosphocholine (DPC) micelles [25]. **1R1M** X-ray structure of the OmpA-like domain of RmpM from *Neisseria meningitidis*, homologous to the C-terminal domain of *E. coli* OmpA [44].

domain of OmpA is composed of ~150 residues, is thought to be globular and is located in the periplasmic space. Although the structure of this domain is not known, the crystal structure of an equivalent fragment from the homologous OMP, RmpM, from *Neisseria meningitidis* has been determined (Fig. 1C). This so-called OmpA-like domain is composed of a mixed β-sheet flanked by two long α-helices. The structure features a hydrophilic groove that could accommodate a peptidoglycan chain. Structural homologues of OmpA have been identified in other species, e.g. OprF from *Pseudomonas aeruginosa* and PmOmpA from *Pasteurella multocida*.

OmpA is ubiquitous in *E. coli* cells with around 100,000 copies found in each cell. OmpA homologues are also expressed at high levels in almost all Gram-negative bacteria. Consequently there is a wealth of experimental data concerning the protein structure and its interactions with the surrounding environment, making it an ideal test case for a study of the dynamics and environmental interactions of outer membrane proteins.

One approach which may be adopted to explore the conformational dynamics of membrane proteins is that of molecular dynamics (MD) simulations [11,12]. MD simulations have been employed as a computational tool to study the conformational dynamics of a wide range of membrane proteins [13,14]. For example, they have been applied with some success to analysis of possible transport mechanisms of ABC transporters [15] and of lactose permease [16]. In this article we review the influence of the local environment on OmpA dynamics as revealed by MD simulations, and the relationship of dynamic behaviour to the function of OmpA and its homologues.

2. Environmental influences on OmpA dynamics

Structural and biophysical studies of OMPs in general subject the proteins to an environment which mimics, but differs from, that present in vivo. OMP structures may be determined either with the protein in a crystal (often in the presence of some detergent molecules) or with the protein solubilised in a detergent micelle (e.g. solution NMR). Both of these environments differ from a bacterial outer membrane. Thus to compare experimental structural data from different sources and to extrapolate to OMPs in their native environment, an understanding of the conformational dynamics of these proteins as a function of environment is required. OmpA is an ideal candidate for such analysis, as it has been studied extensively, both experimentally and via MD simulations.

2.1. Simulations of OmpA in detergent micelles and lipid bilayers

Comparative simulations of the crystal structure of OmpA (PDB code 1BXW) embedded in a lipid bilayer and in a detergent micelle (Fig. 2A, B) have been performed [17,18]. These simulations revealed an enhanced degree of flexibility of the protein in the micelle environment. Using the Cα atom root mean square deviation (RMSD) to measure drift in conformation from the initial structure of a simulation shows that the RMSD for OmpA in a lipid bilayer was comparable to simulations of other membrane proteins in lipid bilayers [19,20], reaching a plateau value of ~2 Å after 2 ns. In contrast, the Cα RMSD in the micelle environment was ~4 Å after 2 ns and drifted to ~5 Å over the subsequent 8 ns. Decomposition of RMSD values into contributions from the various structural elements of OmpA revealed the β-barrel to have the lowest RMSD in both environments, whilst the extracellular loops contributed most to the overall RMSDs. The final protein structures from the two simulations exhibited significant differences. Whilst the conformation of OmpA in a DMPC (dimyristoyl-phosphatidylcholine) bilayer resembled the X-ray structure with the extracellular loops projecting away from the protein and membrane, in the final conformation of the OmpA/DPC (dodecyl-phosphocholine) micelle simulation the loops have 'opened up', yielding a structure that was somewhat closer to the NMR structure.

The interactions of OmpA with the surrounding environment were characterised in both the micelle and bilayer simulations. Density profiles of both systems were analysed to yield the widths of the zones of hydrophobic interaction between protein and detergent /lipid. Estimates of ~45 Å were obtained for both the bilayer and the micelle simulations, indicating a comparable extent of interaction of the central hydrophobic protein surface with both lipids and detergents. The width, along the barrel axis,

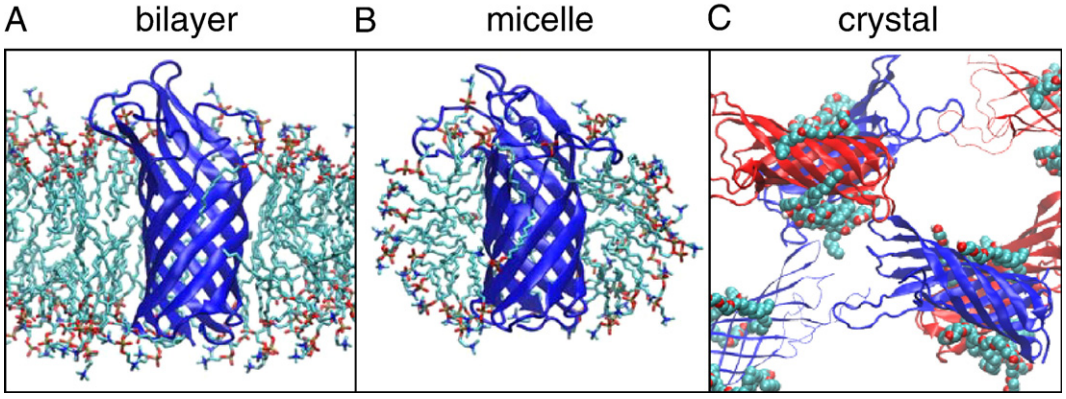

Fig. 2. MD simulations of OmpA vs. environment. (A) Lipid (DMPC) bilayer; (B) detergent (DPC) micelle; and (C) crystal (corresponding to PDB id 1QJP).

of the interfacial region in the OmpA–DMPC system was ~13 Å on the periplasmic side and ~16 Å on the extracellular side. The corresponding values in the OmpA–DPC system were ~14 Å on both sides. At the extracellular end of the barrel there was a significantly broader region of polar headgroup density in the detergent micelle simulation compared to the lipid bilayer simulation.

Analysis of the protein–lipid/detergent hydrogen-bonding (H-bonding) and protein solvent-accessible surface area patterns revealed interesting differences in the two environments. It appears that OmpA formed tighter and more specific interactions with the detergents compared to the lipid molecules, as reflected in a reduced protein solvent accessible surface area and a greater number of protein–detergent H-bonds (and consequently a lower number of protein–water H-bonds). Specifically by the end of the simulations there were 42 protein–DPC H-bonds in the micelle compared to only 15 protein–DMPC H-bonds in the bilayer system. The interactions of the extracellular loops contributed the greatest differences in behaviour between the two systems. Their intrinsic flexibility enabled them to form significantly more interactions with the surrounding detergent molecules in the micelle. In contrast, the mobility of the loops was more restricted in the lipid bilayer environment.

Whilst these simulations were initiated from structures of the pre-inserted protein, MD studies have also been performed to study spontaneous DPC micelle formation around OmpA [17,18]. A similar MD study of the small outer membrane protein OmpX from *E. coli* in dihexanoylphosphatidylcholine (DHPC) detergent micelles was reported by Bockmann and Caflisch [21]. These simulations enabled unbiased determination of the arrangement of detergent molecules around the protein and explored how they might influence its conformational dynamics.

2.2. Simulations of OmpA in a crystal unit cell

Although most OMP structures have been determined by X-ray diffraction, relatively little is known concerning the conformational dynamics of protein–detergent and protein–protein interactions within such crystals. OmpA has been used as a model system for the first MD simulation study of a membrane protein in its crystal environment [22]. The crystallographic unit cell simulated contained 4 OmpA molecules, 24 *n*-octyltetraoxyethylene (C_8E_4) detergent molecules, and water (Fig. 2C). A 50 ns duration simulation, performed at 300 K, provided an atomic level description of the structure and dynamics of detergent and protein molecules within the crystalline environment at the temperature required for crystallization but preceding flash-cooling. This provided insights into the stabilizing forces between protein and detergent associated with the formation and maintenance of the crystal.

A key finding of these studies was the high degree of correlation between residue-by-residue fluctuations in the simulation and experimental crystallographic B-factors. This suggests that the simulations reproduced accurately the protein dynamics within the crystal. The structural integrity of the unit cell was maintained as a result of three types of contacts. Two of these were between adjacent β-barrels, mediated by an annular layer of C_8E_4 detergent molecules, whilst a third, smaller interaction involved direct protein–protein contacts between the loops and turns of pairs of OmpA chains. The conformational flexibility of each individual OmpA monomer in the unit cell was rather low. Thus, the Cα RMSD of each of the β-barrels was less than 2 Å, even after 50 ns. This is comparable to the degree of β-barrel flexibility observed in a detergent micelle, although slightly higher than in a lipid bilayer. For the whole protein (i.e. inclusive of loop/turn regions), the Cα RMSD reached a plateau value of ~3.5 Å after 50 ns. Thus, in contrast with the stability of the β-barrel, the extracellular regions of the protein were more stable than in a detergent micelle (RMSD ~4.5 Å), whilst still higher than in the bilayer environment (RMSD ~2 Å). This conformational stability is primarily a consequence of the reduced mobility of the extracellular loops, due to the well-maintained crystal contacts described above. Finally, it should also be noted that the RMSD of the four OmpA trajectories averaged over time was much smaller than for the individual monomers, as a result of cancellation of random deviations. This implies that analysis of multiple trajectories (or of a greater number of unit cells) may improve agreement with experiment, since electron density from a crystal structure is, similarly averaged.

From a functional perspective, the β-barrel core structure was well maintained throughout the 50 ns simulation in the crystal. Consequently, the proposed 'gate' region (see below) prevented water molecules from traversing the pore of any of the four OmpA molecules in the unit cell. Thus, despite a comparable degree of protein flexibility of the β-barrel to the micelle simulation, pore formation was not seen. This implies that the flexibility of the extracellular loops may have a role in gating, as has been shown for other OMPs [23].

Consistent with this hypothesis, principal components analysis revealed small movements perpendicular to the barrel axis which appeared to be elastically propagated from more significant vibrations in the loops. These vibrations, or 'breathing motions', were consistent with the experimentally observed anisotropic B-factors [24], and with dynamic data from solution NMR studies [25]. Thus, evidence from both theoretical and structural techniques reveal a common pattern for the conformational flexibility of a so-called simple β-barrel membrane protein.

The simulation also allowed the dynamic behaviour of detergent in a crystal unit cell to be described. Over the 50 ns period, the C_8E_4 molecules remained bound to the protein surfaces, primarily between the β-barrels of adjacent OmpA molecules. Individual detergent molecules were shown to be rather mobile, with comparable lateral diffusion coefficients to those of lipids bound to OmpA in a bilayer simulation of a crystal unit cell. However, the lack of a tightly-packed hydrophobic core (in contrast with a bilayer) combined with the more uniform, polar nature of C_8E_4 detergent molecules (compared to lipids) resulted in translational diffusion of detergents along the entirety of the OmpA crystallographic 'fibres'. Thus, a picture emerges of an interconnected micelle-like detergent network, as suggested by neutron diffraction studies of other OMPs [26], in

contrast to the annular lipids often implied to be associated with membrane proteins in their native environment.

3. OmpA gating: an electrostatic switch mechanism?

In addition to a structural role for OmpA in the outer membrane of Gram-negative bacteria, it also forms ion permeable pores. In support of this, physiological studies indicate that OmpA pores can substitute for porins when *E. coli* cells are subjected to osmotic stress [27]. Furthermore, the homologous OprF (see below) is the major porin (i.e. replaces porins such as OmpF and OmpC) in *P. aeruginosa* [27,28]. OmpA (and homologues such as OprF) have come to be classified as "slow porins". This is because, upon reconstitution into proteoliposomes, OmpA [27,28] and OprF [27,28] produce non-specific diffusion channels for various solutes, whose *sizes* would suggest the channels are comparable in diameter to the *E. coli* porins OmpF and OmpC, but whose *rates* of penetration for those solutes were much lower (by about 2 orders of magnitude). This apparent paradox of "low permeability through a large channel" [27,28] was explained by the demonstration via sedimentation experiments that populations of OmpA [27,28] or OprF [29] monomers in unilamellar proteoliposomes consist of two alternative conformers, a majority (>90%) containing "closed" channels and a minority containing "open" channels. Interestingly, an open channel-enriched fraction revealed several conductance substates [30]. Sugawara et al. also performed directed proteolysis and biotin labelling experiments [29] to show that the majority conformer is the "canonical" OmpA-like, two-domain structure, whereas the minority, "open" conformer may exist as a single domain, possibly a larger 16-stranded β-barrel.

Although this two-conformer model may explain the "slow porin" paradox, it does not tell the whole story. Thus, several groups have reported the formation of ion permeable pores in vitro by the intact OmpA protein (i.e. both the N- and C-terminal domains) [31–34], with a range of conductance levels. Most recently, full-length OmpA (and several mutants) could form both small (~50 pS) and large (~300 pS) channels, which were interchangeable on a millisecond timescale, as reflected by their "flickering" conductances [27,28]. Most significantly, the isolated N-terminal domain was also able to form channels, but only at the lower conductance states [27,28]. Thus, the smaller channels correspond to the N-terminal domain, whilst both domains are required to form the larger channels and presumably correspond to a different in vitro conformation of OmpA. Similar behaviour has been observed for OprF, although the two conductance states were larger [39]. Clearly, the demonstration of pore formation by the isolated N-terminal domain requires modification of the two-conformer "closed vs. open" model described above. Moreover, the reversible transitions between small- and large-conductance channels for the full-length protein occur on a millisecond timescale, and so are highly unlikely to be explained by the near-complete unfolding/refolding required for interconversion between a two-domain, 8-stranded and single-domain, 16-stranded β-barrel. This suggests that a "higher-order" model may be necessary to explain the channel behaviour for OmpA and its homologues: This would require two stably folded conformers, one possibly corresponding to (i) a large, porin-like β-barrel, and the other corresponding to (ii) the canonical OmpA structure with an N-terminal, β-barrel domain and a C-terminal, α-helical globular domain, but which is (iii) still associated with smaller conductance states, between which subtle conformational transitions may occur on a millisecond timescale.

Examination of the crystal structure of the N-terminal domain of OmpA (PDB code 1BXW) begins to provide molecular-level clues to the subtle transitions required for channel formation associated with these smaller conductance states. The structure reveals ~20 water molecules inside the transmembrane β-barrel, which form three distinct groups. However, there is not a continuous channel that spans the length of the barrel in the crystal structure. This suggested that changes in OmpA structure would be required to open a transmembrane pore.

MD simulations of the OmpA N-terminal domain embedded within a DMPC bilayer combined with molecular modelling studies have been used to propose a gating mechanism for OmpA [35]. Water molecules were observed to penetrate into the transmembrane β-barrel from both the periplasmic and extracellular sides. However none of the water molecules was observed to traverse the entire barrel. Thus, the X-ray structure of OmpA was confirmed to be functionally closed.

More detailed examination of the closed pore simulation revealed a degree of expansion of the barrel, especially at the extracellular and periplasmic mouths. In particular, although a H-bond between the barrel and the N-terminal periplasmic 'cover', formed by residues 1–4 (which had been proposed to block entry from the periplasmic mouth [36]) was observed in all of the simulations, substantial mobility of residues 1–4 allowed widening of the pore in this region. Similarly, on the extracellular side of the protein significant mobility leading to conformational deviations from the crystal structure was observed for the complex network of hydrophilic residues making up the 'polar ring'. Nevertheless, analysis of the simulated pore dimensions revealed a region too narrow (radius < 1.15 Å) to accommodate a single water molecule, corresponding to the salt bridge formed by residues R138–E52. This salt bridge persisted throughout the closed state simulations and provided the main barrier to water molecules permeating the pore. Whilst the dynamic behaviour observed in the simulations suggested that the pore might be able to adopt a different conformation from the crystal structure, the timescale of the simulations (10 ns) was too short to reveal such a conformational change. Thus, to test the possibility of an alternative conformation of OmpA, a model of the pore in the 'open' state was constructed. Based on analysis of the pattern of H-bonding within the pore it was suggested that R138 could form alternative H bonds with either E128 or E52. A model of OmpA in which the R138 sidechain was rotated towards E128 (rather than E52 in the crystal structure) was generated. MD simulations of this putative open state revealed water permeation events within ~2 ns. Furthermore, approximate estimates of the conductance based on the 'open state' pore dimensions agreed well with the experimentally measured conductance for the N-terminal domain of OmpA. Thus it was proposed that a model

for the 'open' conformation of OmpA could be based on an alternative pattern of H-bonding of R138 (Fig. 3A) In simulations of OmpA in a detergent micelle a conformation 'intermediate' between the closed and fully open state was observed. An alternative rotamer was observed for R138, which resulted in it moving closer to E128. Thus, in the micelle environment, R138 seemed to be interacting with both E52 and E128. This was enough to allow passage of some water molecules, unlike in the bilayer environment.

Recent experimental studies of OmpA have confirmed the position of the gate [27]. Interaction energies of charged and polar sidechains within the β-barrel were assessed by double-mutant cycle analysis and correlated with channel activities of the corresponding point mutants. Their analysis revealed the R138–E52 salt bridge in the OmpA crystal structure did indeed form the main barrier for ion passage into the β-barrel of OmpA (Fig. 3B). The residues identified by Tamm et al. [27] as key in the electrostatic gating of OmpA were E52, R138 and K82 compared to E52, R138 and E128 identified by Bond et al. [35]. Thus the experimental and simulation studies are in broad agreement in identifying a key region of the OmpA structure as an 'electrostatic gate' [37]. MD studies of the gating mechanisms of outer membrane proteins also include exploration of possible mechanisms of the voltage-dependent gating of the trimeric protein OmpF [38].

4. Modelling and simulations of OmpA homologues

To extend our understanding of the structure/function relationships to OmpA homologues (orthologues) from other species of bacteria, it is important to be able to build and assess accurate homology models of these proteins. As an example of this process, we will consider OprF, an OmpA orthologue from *P. aeruginosa*. OprF and *E. coli* OmpA share 39% sequence identity and 56% similarity in their C-terminal domains, but only 15% identity in their N-terminal (TM) domains. OprF has been suggested to have a dual role, as a transbilayer pore and as a structural protein important for the maintenance of cell shape and growth on low-osmolarity media [39]. As with OmpA, OprF has been shown to form pores with more than one conductance level, and pore formation has been reported for the isolated N-terminal domain [40], [41]. Homology models of OprF have been proposed by Brinkman et al. [41] and by Khalid et al. [42], both using the OmpA crystal structure as a template and suggesting that OprF may form a narrow, OmpA-like pore. Simulations based on both models revealed a degree of flexibility in the 'pore', although a continuous pore was not observed. There were three regions of constriction in the pore, formed by H-bonds between residues Y51 and H95, E8 and K121, to a lesser extent by E10 and Y88. To investigate the stability of the H-bonds between residues that constrict the pore, a further simulation was performed in which water molecules were placed in the cavities in the pore prior to simulation. Analysis of this trajectory revealed the pore to be constricted only by E8 and K121. Water molecules were observed to pass through the regions constricted by Y51–H95 and E10–Y88 in the previous simulations. Thus, the most persistent region of constriction was formed by the E8–K121 salt bridge; the authors noted that this constriction is similar to the proposed gate region in OmpA (Fig. 4).

These studies have demonstrated that conformationally stable models of the TM domain of OmpA homologues may be generated and used as the basis of simulations to further probe structure/function relationships. It is therefore of interest to explore whether modeling approaches can be extended to intact, multi-domain OmpA homologues.

PmOmpA is the major protein of the outer membrane of *P. multocida* (a pathogenic species of some economic

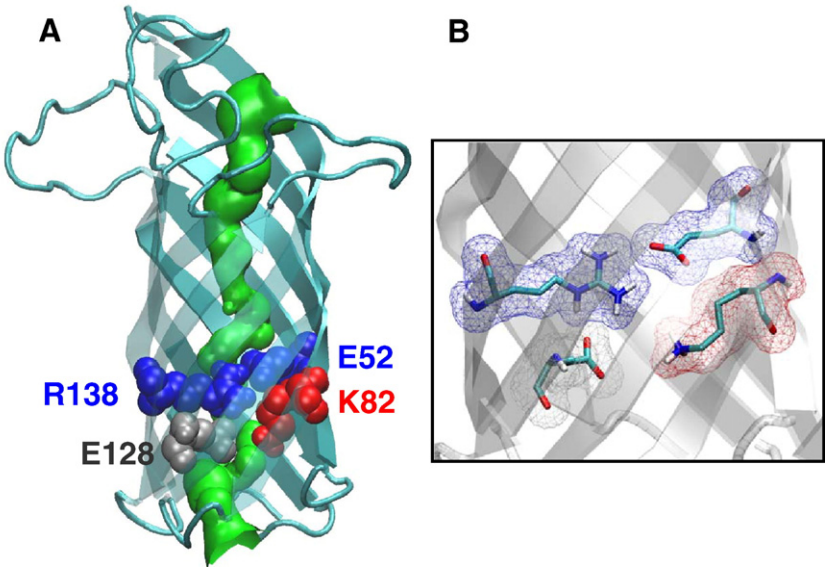

Fig. 3. OmpA pore gating. (A) Structure from the simulation of OmpA in a detergent micelle, showing the pore-lining surface (calculated using HOLE [49]) in green. The sidechains forming the electrostatic gate are shown in spacefilling format, using the following colour code: red = implicated in gating by Tamm et al. [27]; silver = implicated by Bond et al. [35]; blue = implicated by both Tamm et al. and by Bond et al. (B) The key sidechains of the electrostatic gate, colour coded in the same manner as in panel A.

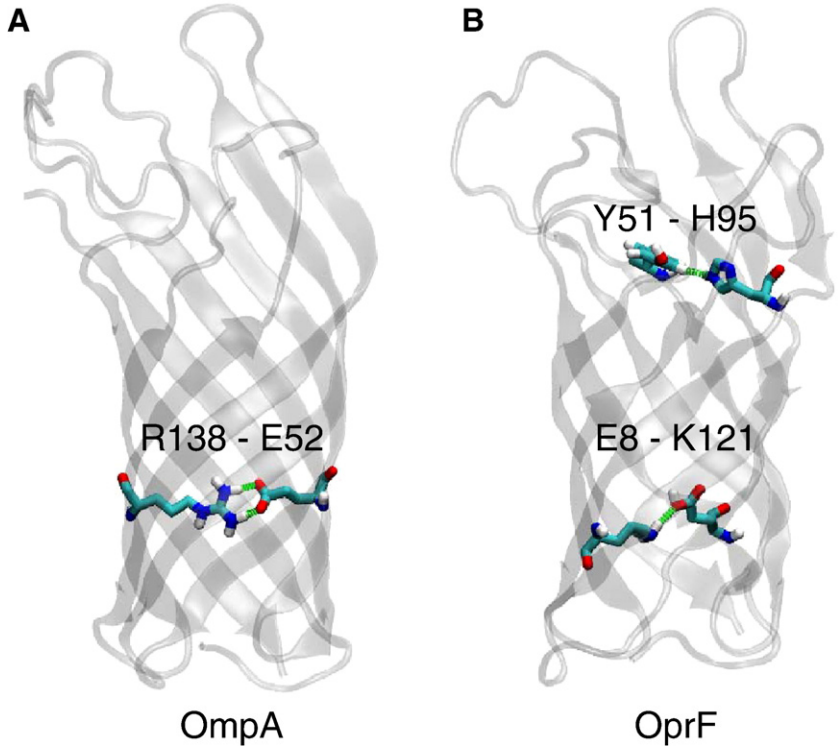

Fig. 4. Comparison of (A) OmpA and (B) OprF, showing the putative gates formed by electrostatic interactions and/or H-bonds across the interior of the β-barrel.

importance) [43], and is a structural homologue of OmpA from *E. coli*. The N-terminal domain of PmOmpA shares a 40% identity with *E. coli* OmpA, for which a structure is known (PDB code 1BXW), and the C-terminal domain shares a 40% sequence identity with the *N. meningitidis* RmpM C-terminal domain, for which a structure is also known (Fig. 1; PDB code 1R1M) [44]. A short (relative to the 18 residue linker of *E. coli* OmpA), 4-residue linker connects the two domains. This makes PmOmpA an ideal case for a study into more complex, multi-domain OMPs.

The linker region was modelled by treating the linker sequence as an extension of both the N- and C-terminal structures (modelled from 1BXW and 1R1M respectively). Thus two ensembles of linker structures were created as extensions, one ensemble from each template. Analysis of the two ensembles revealed the linker conformations with the lowest energies to be similar (Cα RMSD of only 0.4 Å). The linker model with the lowest energy overall was from the ensemble modelled as an extension of the C-terminal domain. The most suitable C-terminal model, identified using Procheck [45], with the linker region present, was manually docked onto the N-terminal domain model. The model of the intact protein was then subjected to energy minimisation to optimise the geometry of the linker.

This multi-domain system was then embedded in a DMPC bilayer, equilibrated, and simulated for 20 ns under two different salt concentrations conditions: neutralising amounts of counter-ions (low), and at ~1 M NaCl solution (high). Analysis of the conformational drift provides insights into both the stability of the component domains, and of their movements relative to one another. Cα RMSDs of the N-terminal domains in both low and high salt concentrations plateau quickly (after ~1.5 ns) to ~2.3 Å and ~2.4 Å respectively (~1.30 Å and ~1.25 Å for the β-barrel regions). However, the C-terminal domains plateau after ~1.5 ns to ~2.9 Å in low salt and after ~4.5 ns to 4.2 Å in high salt. The secondary structure elements of the whole protein remain stable throughout the simulation. Not only does the linker region stay as a random coil, but the secondary structure elements around it retain their integrity. In both simulations the RMSD for the whole PmOmpA structure rises to a higher plateau and shows bigger fluctuations than for the two individual domains (~10.5 Å for low salt and ~6.5 Å for high salt). The fluctuations in RMSD of the whole molecule indicate significant inter-domain motion, which is more pronounced in low salt. Visualisation of the two simulations confirms this. The Cα atom root mean square fluctuation (RMSF) can be used to measure the protein flexibility. The RMSF profile for the protein in both simulations shows a slightly higher average for the C-terminal domain (~1.4 Å) compared to the N-terminal domain (~1.0 Å), as might be expected for a globular domain relative to a transmembrane β-barrel.

Both visual analysis of the simulations and calculation of eigenvectors confirm that the C-terminal domain moves substantially relative to the bilayer-embedded N-terminal domain. In the low salt simulation this is manifested as a movement of the C-terminal domain towards the inner leaflet of the bilayer, whereas in the high salt simulation the dominant motion is a 'twisting' of the domains relative to one another (Fig. 5).

To further evaluate the movement of the C-terminal domain in each simulation, the lipid–protein interactions were analysed.

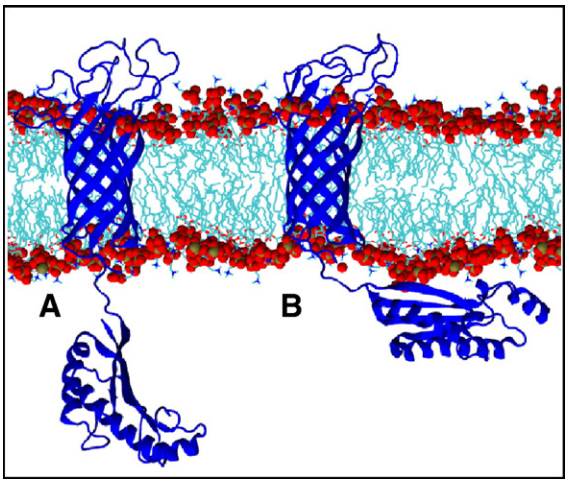

Fig. 5. PmOmpA: simulations of a homology model of an intact OmpA molecule. The structure at the start (A) and end (B: 20 ns) of a simulation of PmOmpA in a DMPC bilayer showing the change in orientation of the periplasmic domain such that it interacts with the surface of the bilayer.

The total number of lipid–protein interactions (defined by a distance cutoff of 3.5 Å) were calculated as a function of time. Both simulations plateau and fluctuate at around ~400 interactions after ~6 ns. The high salt simulation remains at about this value for the remainder of the 20 ns. After ~10 ns in the low salt simulation the number of interactions jumps to ~500. These additional interactions were due to the C-terminal domain moving to such an extent that it contacts the inner leaflet of the bilayer. As the movement is not as pronounced in the high salt simulation, these interactions do not occur. If we consider just the N-terminal domain and the lipid head groups then the number of lipid protein interactions for the low salt simulation fluctuates around ~180. These values are comparable to those reported for the N-terminal domain homology model of OprF [42], suggesting conservation of overall lipid–protein interactions between homologues. The nature of the lipid–protein interactions (for both domains) was monitored by further analysing the number of interactions as a function of time and position along the bilayer normal. In both simulations, two distinct bands of interactions corresponding to the head group regions of the bilayer were observed. A third band of interactions was observed on the periplasmic side of the lipid bilayer in the low salt simulation. This band corresponds to the interactions of the C-terminal domain. The lack of such a third band from the high salt simulation reflects the lack of movement of the C-terminal domain towards the lipid bilayer. To understand the reasons for the differences in movement of the C-terminal domain, the interactions were analysed in more detail. The majority of the C-terminal contacts with the lipid bilayer occurred between charged/polar residues and the lipid head groups. In fact, six of the ten C-terminal domain residues that interact most with lipids are charged. Thus the interactions of the C-terminal domain with the bilayer are largely electrostatic, and in the presence of 1 M NaCl these electrostatic attractions are shielded by the Na^+ and Cl^- ions. This reduced attraction results in the decreased movement of the C-terminal domain towards the bilayer.

5. Conclusions and outlook

The abundance of experimental data characterizing the structure and dynamics, in various environments, of the outer membrane protein OmpA from *E. coli* make it an ideal test case for a study of the dynamics and environmental interactions of outer membrane proteins. MD simulations of OmpA in lipid bilayers, detergent micelles and in a crystalline environment have enabled comparison of the protein dynamics in environments that mimic experimental conditions. Such simulations have helped to explain apparently conflicting experimental observations concerning the pore-like properties of OmpA. Moreover the gating region of OmpA was identified by simulations in advance of experimental evidence identifying the same region.

MD simulation studies have been extended to OmpA-homologues from other organisms. Simulations based on homology models of OmpA-homologues whose structure is unknown have been used to study multi-domain models. Homology modelling and simulations of the OmpA homologue, OprF, the main porin of *P. aeruginosa* suggested this protein has a similar electrostatic gating mechanism to OmpA. Simulations of the multi-domain homology model of the PmOmpA protein from *P. multocida* have provided insights into the dynamics and environmental interactions of the intact protein. Substantial interaction of the periplasmic domain with the lipid bilayer was observed under low salt conditions but not in high salt conditions. The main constriction in the transmembrane barrel domain of PmOmpA was formed by an Arg–Glu salt bridge located in a similar position to the Arg–Glu salt bridge identified as the gate region by simulation and experimental studies of OmpA. Thus the homologues, OmpA (*E. coli*), OprF (*P. aeruginosa*) and PmOmpA (*P. multocida*) may be gated by salt bridges located within the β barrel, and this opens up the question of whether small OMPs share a similar mechanism of gating [23].

The simulations reviewed in this article have demonstrated the ability of MD to complement experimental techniques in providing a more comprehensive view of the dynamics of OmpA and its homologues under different environmental

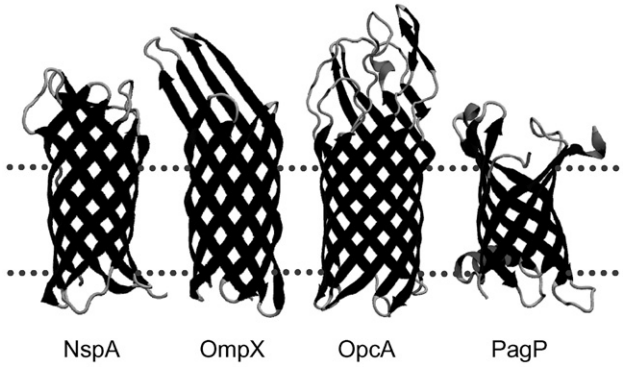

Fig. 6. Other 'simple' OMPs that have been the subject of MD simulation studies: NspA (PDB code 1P4T), OmpX (PDB code 1QJ8), OpcA (PDB code 1K24), and PagP (PDB code 1THQ). The dotted line indicates the approximate extent of the lipid bilayer.

conditions. However, to date, the outer membrane environment in simulations of OMPs has always been represented by a phospholipid bilayer. This is a simplified model of the bacterial outer membrane which is composed of lipopolyaccharide (LPS) in the outer leaflet and phospholipids in the inner leaflet. In-depth understanding of the interactions of OMPs in their native environment will require a more detailed model of the OM featuring LPS in the outer leaflet and phospholipids in the inner leaflet. Whilst simulations of such an atomistic model have been reported [46], none have been reported with an embedded OMP. These simulation methods can be extended to a range of other OMPs [6–10,47,48] (Fig. 6). Together with a more detailed representation of the lipid content of the outer membrane will allow the construction of a 'virtual outer membrane'.

Acknowledgements

This work was supported by grants from the BBSRC, the EPSRC (via the Bionanotechnology IRC), and the Wellcome Trust.

References

[1] W.C. Wimley, The versatile β-barrel membrane protein, Curr. Opin. Struct. Biol. 13 (2003) 404–411.
[2] G.E. Schulz, The structure of bacterial outer membrane proteins, Biochim. Biophys. Acta 1565 (2002) 308–317.
[3] H. Nikaido, Molecular basis of bacterial outer membrane permeability revisited, Microbiol. Mol. Biol. Rev. 67 (2003) 593–656.
[4] C.R. Raetz, C.M. Reynolds, M.S. Trent, R.E. Bishop, Lipid A modification systems in gram-negative bacteria, Annu. Rev. Biochem. 76 (2007) 295–329.
[5] C.R. Raetz, C. Whitfield, Lipopolysaccharide endotoxins, Annu. Rev. Biochem. 71 (2002) 635–700.
[6] P.M. Hwang, W.Y. Choy, E.I. Lo, L. Chen, J.D. Forman-Kay, C.R.H. Raetz, G.G. Privé, R.E. Bishop, L.E. Kay, Solution structure and dynamics of the outer membrane enzyme PagP by NMR, Proc. Natl. Acad. Sci. U. S. A. 99 (2002) 13560–13565.
[7] P.M. Hwang, R.E. Bishop, L.E. Kay, The integral membrane enzyme PagP alternates between two dynamically distinct states, Proc. Natl. Acad. Sci. U. S. A. 101 (2004) 9618–9623.
[8] V.E. Ahn, E.I. Lo, C.K. Engel, L. Chen, P.M. Hwang, L.E. Kay, R.E. Bishop, G.G. Privé, A hydrocarbon ruler measures palmitate in the enzymatic acylation of endotoxin, EMBO J. 23 (2004) 2931–2941.
[9] C. Fernandez, C. Hilty, G. Wider, P. Güntert, K. Wüthrich, NMR structure of the integral membrane protein OmpX, J. Mol. Biol. 336 (2004) 1211–1221.
[10] J. Vogt, G.E. Schulz, The structure of the outer membrane protein OmpX from *Escherichia coli* reveals possible mechanisms of virulence, Structure Fold Des. 7 (1999) 1301–1309.
[11] M.J. Karplus, J.A. McCammon, Molecular dynamics simulations of biomolecules, Nat. Struct. Biol. 9 (2002) 646–652.
[12] S.A. Adcock, J.A. McCammon, Molecular dynamics: survey of methods for simulating the activity of proteins, Chem. Rev. 106 (2006) 1589–1615.
[13] W.L. Ash, M.R. Zlomislic, E.O. Oloo, D.P. Tieleman, Computer simulations of membrane proteins, Biochim. Biophys. Acta 1666 (2004) 158–189.
[14] B. Roux, K. Schulten, Computational studies of membrane channels, Structure 12 (2004) 1343–1351.
[15] E.O. Oloo, D.P. Tieleman, Conformational transitions induced by the binding of MgATP to the vitamin B12 ATP-binding cassette (ABC) transporter BtuCD, J. Biol. Chem. 279 (2004) 45013–45019.
[16] Y. Yin, M. Jensen, E. Tajkhorshid, K. Schulten, Sugar binding and protein conformational changes in lactose permease, Biophys. J. 91 (2006) 3972–3985.
[17] P.J. Bond, J.M. Cuthbertson, S.D. Deol, M.S.P. Sansom, MD simulations of spontaneous membrane protein/detergent micelle formation, J. Am. Chem. Soc. 126 (2004) 15948–15949.
[18] P.J. Bond, M.S.P. Sansom, Membrane protein dynamics vs. environment: simulations of OmpA in a micelle and in a bilayer, J. Mol. Biol. 329 (2003) 1035–1053.
[19] D.P. Tieleman, H.J.C. Berendsen, A molecular dynamics study of the pores formed by *Escherichia coli* OmpF porin in a fully hydrated palmitoyloleoylphosphatidylcholine bilayer, Biophys. J. 74 (1998) 2786–2801.
[20] J.D. Faraldo-Gómez, G.R. Smith, M.S.P. Sansom, Molecular dynamics simulations of the bacterial outer membrane protein FhuA: a comparative study of the ferrichrome-free and bound states, Biophys. J. 85 (2003) 1–15.
[21] R.A. Böckmann, A. Caflisch, Spontaneous formation of detergent micelles around the outer membrane protein OmpX, Biophys. J. 86 (2005) 3191–3204.
[22] P.J. Bond, J.D. Faraldo-Gómez, S.S. Deol, M.S.P. Sansom, Membrane protein dynamics and detergent interactions within a crystal: a simulation study of OmpA, Proc. Natl. Acad. Sci. U. S. A. 103 (2006) 9518–9523.
[23] P.J. Bond, J.P. Derrick, M.S.P. Sansom, Membrane simulations of OpcA: gating in the loops? Biophys. J. 92 (2007) L23–L25.
[24] A. Pautsch, G.E. Schulz, High-resolution structure of the OmpA membrane domain, J. Mol. Biol. 298 (2000) 273–282.
[25] A. Arora, F. Abildgaard, J.H. Bushweller, L.K. Tamm, Structure of outer membrane protein A transmembrane domain by NMR spectroscopy, Nat. Struct. Biol. 8 (2001) 334–338.
[26] H.J. Snijder, P.A. Timmins, K.H. Kalk, B.W. Dijkstra, Detergent organisation in crystals of monomeric outer membrane phospholipase A, J. Struct. Biol. 141 (2003) 122–131.
[27] H. Hong, G. Szabo, L.K. Tamm, Electrostatic couplings in OmpA ion-channel gating suggest a mechanism for pore opening, Nat. Chem. Biol. 2 (2006) 627–635.
[28] L.K. Tamm, B. Liang, NMR of membrane proteins in solution, Prog. Nucl. Magn. Res. Spectrosc. 48 (2006) 201–210.
[29] E. Sugawara, E.M. Nestorovich, S.M. Bezrukov, H. Nikaido, *Pseudomonas aeruginosa* porin OprF exists in two different conformations, J. Biol. Chem. 281 (2006) 16220–16229.
[30] E.M. Nestorovich, E. Sugawara, H. Nikaido, S.M. Bezrukov, *Pseudomonas aeruginosa* porin OprF: properties of the channel, J. Biol. Chem. 281 (2006) 16230–16237.
[31] E. Sugawara, H. Nikaido, OmpA protein of *Escherichia coli* outer-membrane occurs in open and closed channel forms, J. Biol. Chem. 269 (1994) 17981–17987.
[32] E. Sugawara, H. Nikaido, Pore-forming activity of OmpA protein of *Escherichia coli*, J. Biol. Chem. 267 (1992) 2507–2511.
[33] N. Saint, E. De, S. Julien, N. Orange, G. Molle, Ionophore properties of OmpA of *Escherichia coli*, Biochim. Biophys. Acta 1145 (1993) 119–123.
[34] A. Arora, D. Rinehart, G. Szabo, L.K. Tamm, Refolded outer membrane protein A of *Escherichia coli* forms ion channels with two conductance states in planar lipid bilayers, J. Biol. Chem. 275 (2000) 1594–1600.
[35] P.J. Bond, J.D. Faraldo-Gómez, M.S.P. Sansom, OmpA—A pore or not a pore? Simulation and modelling studies, Biophys. J. 83 (2002) 763–775.
[36] A. Pautsch, G.E. Schulz, Structure of the outer membrane protein A transmembrane domain, Nat. Struct. Biol. 5 (1998) 1013–1017.
[37] O. Beckstein, P.C. Biggin, P.J. Bond, J.N. Bright, C. Domene, A. Grottesi, J. Holyoake, M.S.P. Sansom, Ion channel gating: insights via molecular simulations, FEBS Lett. 555 (2003) 85–90.
[38] K.M. Robertson, D.P. Tieleman, Molecular basis of voltage gating of OmpF porin, Biochem. Cell Biol. Biochim. Biol. Cell. 80 (2002) 517–523.
[39] H. Nikaido, Porins and specific channels of bacterial outer membranes, Mol. Microbiol. 6 (1992) 435–442.
[40] H. Nikaido, K. Nikaido, S. Harayama, Identification and characterization of porins in *Pseudomonas aeruginosa*, J. Biol. Chem. 266 (1991) 770–779.

[41] F.S.L. Brinkman, M. Bains, R.E.W. Hancock, The amino terminus of *Pseudomonas aeruginosa* outer membrane protein OprF forms channels in lipid bilayer membranes: correlation with a three dimensional model, J. Bacteriol. 182 (2000) 5251–5255.

[42] S. Khalid, P.J. Bond, S.S. Deol, M.S.P. Sansom, Modelling and simulations of a bacterial outer membrane protein: OprF from *Pseudomonas aeruginosa*, Proteins, Struct. Funct. Bioinf. 63 (2005) 6–15.

[43] S.M. Dabo, A.W. Confer, R.A. Quijano-Blas, Molecular and immunological characterization of *Pasteurella multocida* serotype A : 3 OmpA: evidence of its role in *P. multocida* interaction with extracellular matrix molecules, Microb. Pathog. 35 (2003) 147–157.

[44] S. Grizot, S.K. Buchanan, Structure of the OmpA-like domain of RmpM from *Neisseria meningitidis*, Mol. Microbiol. 51 (2004) 1027–1037.

[45] R.A. Laskowski, M.W. Macarthur, D.S. Moss, J.M. Thornton, Procheck—A program to check the stereochemical quality of protein structures, J. Appl. Cryst. 26 (1993) 283–291.

[46] R.D. Lins, T.P. Straatsma, Computer simulation of the rough lipopolysaccharide membrane of *Pseudomonas aeruginosa*, Biophys. J. 81 (2001) 1037–1046.

[47] L. Vandeputte-Rutten, M.P. Bos, J. Tommassen, P. Gros, Crystal structure of Neisserial Surface Protein A (NspA), a conserved outer membrane protein with vaccine potential, J. Biol. Chem. 278 (2003) 24825–24830.

[48] S.M. Prince, M. Achtman, J.P. Derrick, Crystal structure of the OpcA integral membrane adhesion from *Neisseria meningitides*, Proc. Natl. Acad. Sci. U. S. A. 99 (2002) 3417–3421.

[49] O.S. Smart, J.G. Neduvelil, X. Wang, B.A. Wallace, M.S.P. Sansom, Hole: A program for the analysis of the pore dimensions of ion channel structural models, J. Mol. Graph. 14 (1996) 354–360.